Catalysis Letters 20 (1993) 149–157

Theory of EELFS compared with EXAFS for catalysis study

Takashi Fujikawa, Tetsuro Yikegaki [a] and Seiji Usami

Faculty of Engineering, Yokohama National University, Hodogaya, Yokohama 240, Japan
[a] *Advanced Materials Research Laboratory, TOSOH Corporation, Hayakawa, Ayase, Kanagawa 252, Japan*

We discuss the similarity and the difference between EXAFS and EELFS for catalysis study based on the theory developed by the present authors. The information obtained from small- and large-angle scattering EELFS is quite different, and the former setup is recommended for catalysis study.

Keywords: EELFS theory; EXAFS

1. Introduction

In order to understand properties of catalysis the study of surface geometric and electronic structures is very important. For this purpose X-ray absorption fine structures (XAFS) including EXAFS and XANES are now widely used by many authors [1]. These spectroscopies are, however, only accessible at a synchrotron radiation facility. In contrast to this limited accessibility, extended energy-loss fine structure (EELFS) measurement can be easily performed in a laboratory system. This spectroscopy has become a valuable tool for local structural investigation of solid surfaces [2–4].

So far the EELFS analyses have been based on the validity of the dipole approximation which is expected to work well under small-angle scattering condition. In this case EELFS spectra can be analysed with the aid of the conventional EXAFS function $\chi(k)$ to obtain local structural information. When the scattering angle is not so small, we have to look for other simple functions like $\chi(k)$ if possible. However, these are based on the simple theory where the scattering wave functions of a probe electron are approximated by plane waves, that is the Bethe theory [5–7]. To go beyond the Bethe approximation, DeCrescenzi et al. proposed an interesting method based on the distorted-wave Born approximation [8,9]. In their treatment, however, the primary electron wave functions are approximated by crystal Bloch waves. The surface sensitivity of EELFS severely rules out the applicability of such functions.

In this letter we discuss the similarity and the difference between EXAFS and EELFS for surface and catalysis study based on the theoretical framework developed by one of the present authors, which takes the important many-body effects into account.

2. EELFS theory

To use EELFS as a practical tool of surface analyses, it is inevitably necessary to develop a reliable theory to describe inelastic scattering of an electron for any scattering angle. The general theory of the electron scattering from solids has been developed by Fujikawa and Hedin. It describes important many-body effects in a physically transparent and acceptable expression [10]. Based on this theory, a general EELFS theory has been proposed, where important ingredients are damping functions of a probe electron and a secondary excited electron under the influence of the corresponding optical potentials [11].

Using the site T-matrix expansion of the Green's function, we obtain the single-scattering EELFS intensity formula $\hat{A}^1_{11}$ for the excitation from a deep core orbital with angular momentum $(l, m) = (0, 0)$ [11],

$$\hat{A}^1_{11} = \frac{32\pi}{(\Delta p_1)^4} \sum_{\alpha \neq \mathrm{A}} \mathrm{Im}(Z_\alpha) \exp\{-2(l_\mathrm{A} p_2 + l'_\mathrm{A} p'_2)\}\,, \tag{1}$$

where l_A and l'_A are the distance between the excited atom A and the solid surface measured in the direction $\boldsymbol{p}$ (incident momentum) and $\boldsymbol{p}'$ (final momentum), p_2 and p'_2 are the decaying part of the incident and scattered waves of a probe electron due to the influence of the corresponding optical potentials. $\Delta\boldsymbol{p}_1$ is the momentum transfer of the real part of $\boldsymbol{p}$ and $\boldsymbol{p}'$. Because of the damping factors p_2 and p'_2, $\hat{A}^1_{11}$ dominantly reflects the local structure of solid surfaces, which is in contrast to ordinary EXAFS measurements.

The oscillating term as a function of loss energy Z_α is given [11] as

$$Z_\alpha = \exp(2\mathrm{i}kR_\alpha) f_\alpha(\pi) \Gamma_{\alpha\mathrm{A}}(\Delta\boldsymbol{p}_1; k) \Gamma_{\alpha\mathrm{A}}(-\Delta\boldsymbol{p}_1; k)/R^2_\alpha\,. \tag{2}$$

The excitation amplitude $\Gamma_{\alpha\mathrm{A}}(\Delta\boldsymbol{p}_1; k)$ is shown in terms of scattering phase shifts at core excited atom A,

$$\Gamma_{\alpha\mathrm{A}}(\Delta\boldsymbol{p}_1; k) = \sum_l (2l+1) P_l(\cos\theta_\alpha) \rho(l) \mathrm{i}^{-l} \exp(\mathrm{i}\delta^\mathrm{A}_l)\,, \tag{3}$$

where θ_α is the angle between $\Delta\boldsymbol{p}_1$ and $\boldsymbol{R}_\alpha$ and P_l is the Legendre function of lth order. The radial integral $\rho(l)$ is defined by use of the radial wave function $R_l(kr)$ of secondary excited electron with momentum k, and that of core function $R_0(r)$,

$$\rho(l) = \int R_l(kr) j_l(\Delta p_1) R_0(r) r^2 \, \mathrm{d}r\,. \tag{4}$$

The oscillating term Z_α in EELFS is quite similar to the corresponding term $\tilde{Z}_\alpha$ in EXAFS, which is given by [12]

$$\tilde{Z}_\alpha = -9\exp(2ikR_\alpha + 2i\delta_1^A) f_\alpha(\pi)\rho(1)^2\cos^2\theta_\alpha . \tag{5}$$

In the very small Δp limit, we can show that Z_α is reduced to $\tilde{Z}_\alpha$ because of the orthogonality between $R_0(r)$ and $R_l(kr)$. When they use high energy ($\epsilon_p \geqslant 100$ keV) EELFS in transmission mode, this condition is satisfied and they obtain the equivalent EELFS spectra to the corresponding EXAFS spectra.

When we study EELFS spectra in the reflection mode, we should carefully investigate the energy and angular dependence of Z_α [13]. Fig. 1 shows the absolute value of the ratio of $(2l+1)\rho(l)$ to $3\rho(1)$ as a function of a scattering angle for $l = 0$–6, where the fast probe electron (2400 eV) excites an oxygen 1s electron. ϵ_k is 50 eV in fig. 1a and 350 eV in fig. 1b; EELFS measurements are usually carried out for the energy range $\epsilon_k = 50$–350 eV. Since the relative contribution of s-wave $|\rho(0)/3\rho(1)|$ at forward scattering is about 10% for $\epsilon_k = 50$ eV and about 5% for 350

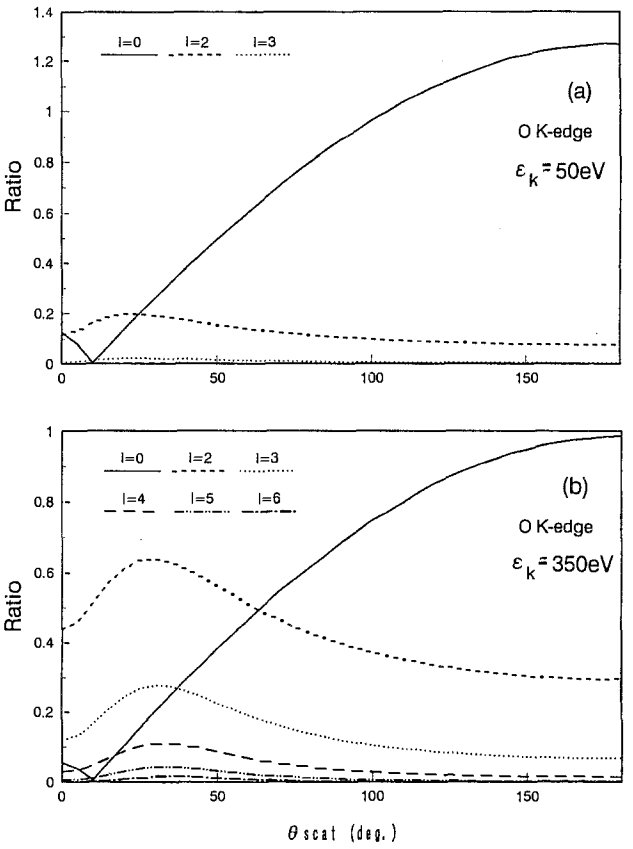

Fig. 1. The ratio $|(2l+1)\rho(l)/3\rho(1)|$ as a function of the scattering angle for $\epsilon_k = 50$ eV (a) and 350 eV (b).

eV, transition to the s-wave cannot be neglected even in the forward scattering in this energy range. As the binding energy of an oxygen 1s orbital is 532 eV, Δp_1 is about 3–5 $Å^{-1}$ corresponding to $\epsilon_k = 50$–350 eV. The wave vector of X-ray plays the same role as Δp_1 in the X-ray absorption whereas it is small, only 0.3–0.5 $Å^{-1}$ in the EXAFS energy region. In contrast to the forward scattering, the s-wave plays a more dominant role for the backscattering. A similar result has been obtained by Tomellini et al. [14]. Furthermore, we can see that $\rho(0)$ happens to vanish at scattering angle of 10°. In the low energy region ($\sim$ 50 eV), the excitation amplitude to the partial waves of $l = 2, 3, \ldots$ becomes negligibly small and that amplitude to the s-wave disappears at this angle, so that the dipole approximation in the sense of the irreducible tensorial expansion works well. Thus we can expect that electron energy loss near edge structure (ELNES) would be equivalent to the corresponding XANES under this condition.

3. Anisotropy

We are very familiar with the polarization dependent anisotropy of EXAFS $\cos^2 \theta_\alpha$ as shown by eq. (5). This simple anisotropic behavior is due to the electric dipole transition approximation. In EELFS, however, several partial waves have nonnegligible contributions to $\Gamma_{\alpha A}$ as described above, so that the phase function of EELFS arg Z_α in eq. (2) is different from that of EXAFS arg $\tilde{Z}_\alpha$. Furthermore this phase function of EELFS depends on the position of surrounding atoms through $P_l(\cos\theta_\alpha)$ as shown in eq. (3). This anisotropy is more complicated than that of EXAFS.

Fig. 2. shows the model O–Ni system used in this calculation. The calculation

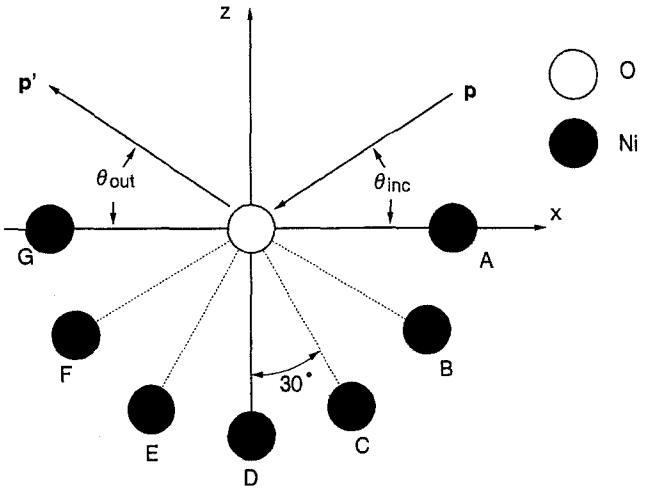

Fig. 2. A model system to study the anisotropy of EELFS: all atoms and $\boldsymbol{p}$ and $\boldsymbol{p}'$ are in the same plane.

has been done for two different modes; the small-angle scattering($\theta_{inc} = \theta_{out} = 5°$) and the back-scattering($\theta_{inc} = \theta_{out} = 90°$). The other parameters are $\epsilon_p = 2500$ eV and $\epsilon_k = 50$–350 eV. Figs. 3a and 3b show the amplitudes and phases of Z_α as a function of the wave number k of the secondary electron for the small-angle scattering. As shown in 3a, the amplitudes are sensitive to the position of the scattering atoms; the atoms E and F have large amplitudes, whereas B and C have small ones. From 3b, we find that the important scatterers like E, F, A, G and D show similar phase curves. This is a desirable result for EELFS analyses. We can expect that the experimental EELFS signal arises mainly from the atoms with large $|\Gamma_{\alpha A}|$ and their phases are nearly the same, so that the single phase function is sufficient for the EELFS analyses.

Figs. 4a and 4b show the amplitudes and phases of Z_α for the back-scattering. From the symmetry consideration, it is enough to show the results for three atoms (D, E and F). Three amplitudes show quite small difference compared with those in fig. 3a. This is due to the fact that $|\rho(0)|$ is important in this large-angle scattering mode as described in section 2. The phase curves in 4b are almost the same, how-

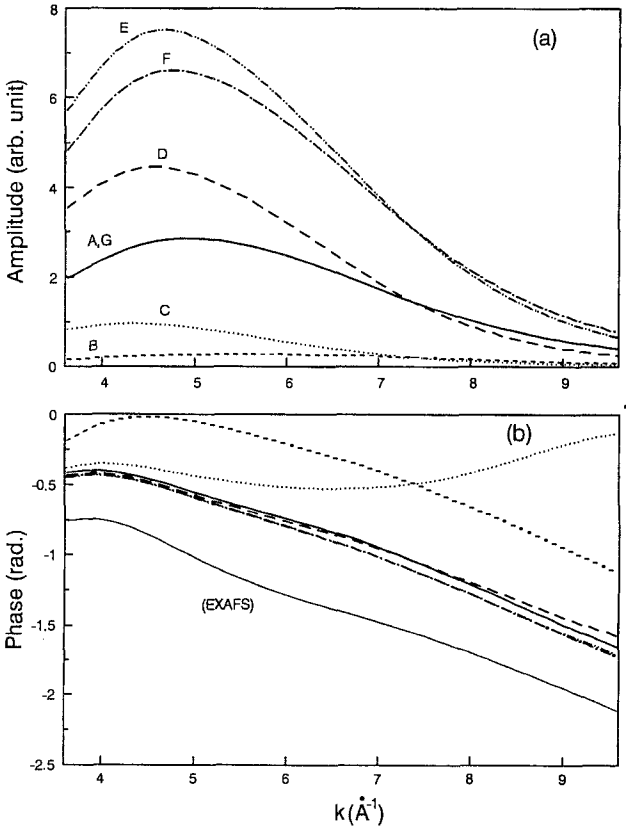

Fig. 3. $|Z_\alpha|$ and arg Z_α as a function of k for each scattering atom A–G as shown in fig. 2; $\theta_{inc} = \theta_{out} = 5°$.

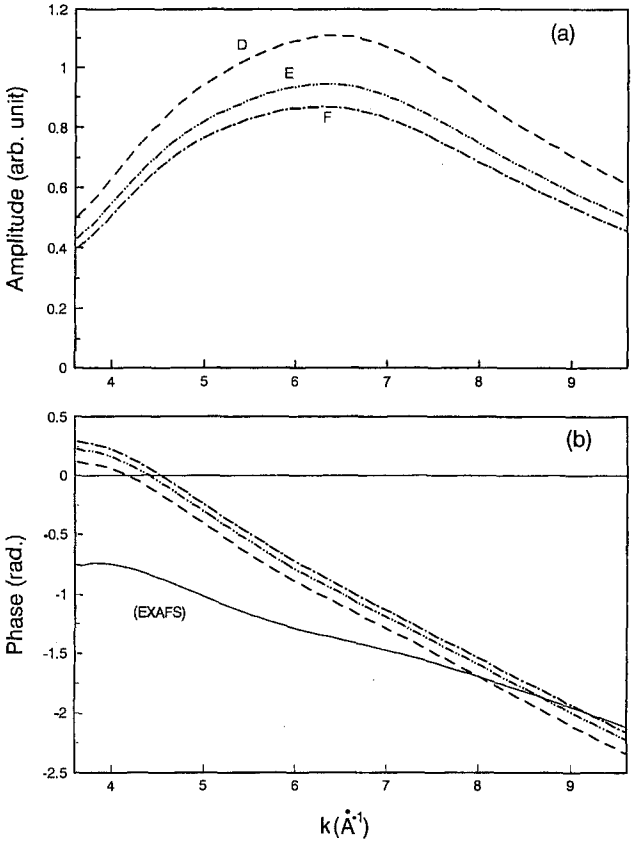

Fig. 4. Same as fig. 3 except the scattering angle; $\theta_{inc} = \theta_{out} = 90°$.

ever, they are clearly different from EXAFS phase curve. Therefore we can conclude that EELFS in the back-scattering mode gives a rather isotropic information about surrounding atoms, and the phase function is different from that of EXAFS.

4. Other oscillations due to elastic scattering of a probe electron

In comparison with X-ray photons, electrons strongly interact with electrons and nuclei in a solid so that probe electrons suffer elastic scattering before and after core excitation even in the EELFS region ($\epsilon_p > 2$–3 keV). This gives rise to an interesting different type of oscillations in energy loss spectra in addition to EELFS oscillation. This type of oscillation is particularly remarkable in large angle scattering [14–16]. These phenomena are explained by the formulas which describe such elastic scattering. For example, energy loss intensity including single elastic scattering after the core excitation is quite similar to the corresponding ARXPS for-

mula, whose energy dependence is mainly affected by $\exp[-iR_\beta p'_1(1-\cos\theta_{p'\beta A})-R_\beta p'_2]$ where $\theta_{p'\beta A}$ is the scattering angle at site β from A to $\boldsymbol{p}'$. When this angle is small enough, we cannot expect such oscillation.

Here we illustrate the calculated results for adsorbed systems p(2 × 2) and c(2 × 2)O/Ni(001), and a single crystalline NiO(001) surface [16]. Adsorbed oxygen atoms are on hollow sites with the shortest O–Ni distance 1.96 Å for both systems. The calculated O K-edge EELS spectra for a probe electron of 2 keV are shown in fig. 5, where (a) [(b)] is a spectrum at $\theta_i = \theta_f = 3°$ [$\theta_i = \theta_f = 90°$]. Here θ_i(incident angle)= θ_{inc}, θ_f(takeoff angle)= θ_{out} are measured from the solid surface. The dotted, dashed and solid lines show the O K-edge EELS spectra for NiO,

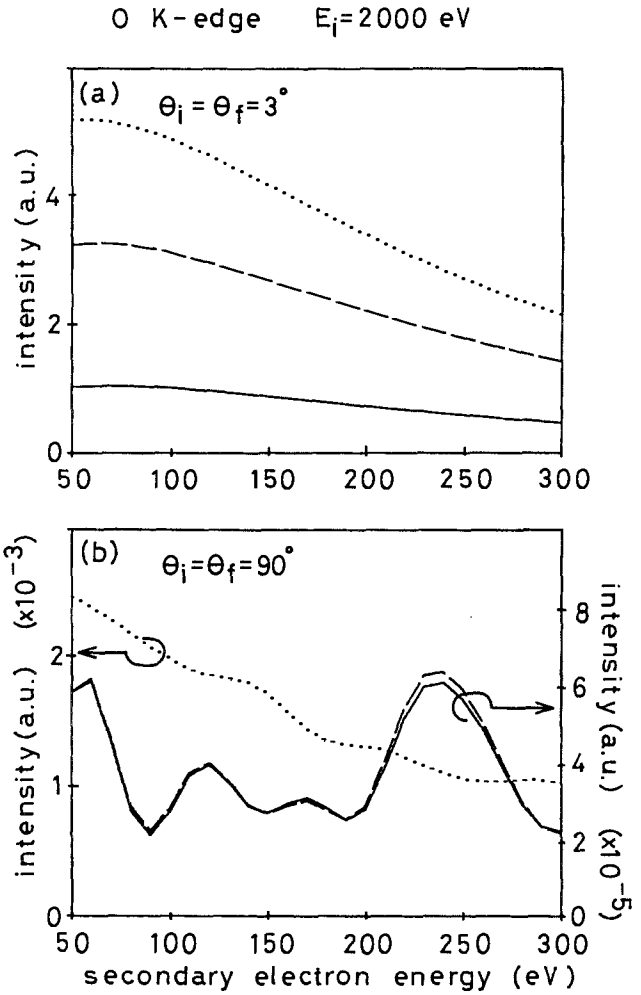

Fig. 5. Calculated EELS spectra for p(2 × 2)O/Ni(001) (solid line), c(2 × 2)O/Ni(001) (dashed line), and NiO(001) (dotted line) surfaces in two detection modes; (a) $\theta_{inc} = \theta_{out} = 3°$, (b) $\theta_{inc} = \theta_{out} = 90°$. The intensities of spectra are normalized to those in (a).

c(2 × 2) and p(2 × 2) surfaces. In the forward scattering shown in fig. 5a, the three spectra are smoothly decreasing functions of ϵ_k. The EELS intensity reflects the density of oxygen atoms in the surfaces. Under this very small-angle scattering condition, the observed EELS is very sensitive to the first layer, and then EELS intensities for the adsorbed systems are not so small compared with that from the oxide surface.

In fig. 5b the EELS spectrum for the NiO surface is quite different from those for c(2 × 2) and p(2 × 2) surfaces, and the spectra for adsorbed systems are nearly the same. The EELS intensity for the oxide surface is about 100 times larger than those for the adsorbed surfaces. In the case of adsorbed systems, if the elastic scattering from the surrounding oxygen atoms, which are in the first layer, mainly contributes to the EELS spectra, we would observe different behavior between them because of the different atomic arrangement around excited oxygen atoms. Therefore the elastic scattering not from O atoms but from Ni atoms in the substrate play an important role in the backward reflection because Ni is a stronger scatterer than O. The atomic configurations between the excited oxygen and Ni atoms are the same in both adsorbed systems, and we find the same EELS spectra for the adsorbed systems.

5. Conclusion

In this letter we have shown that EELFS in the small-angle scattering reflection mode has remarkable features; surface sensitivity, simple theoretical formula from which we can easily get useful local structural information. We can therefore expect that EELFS will be a hopeful tool for catalysis study.

Acknowledgement

Financial support from a Grant-in-Aid for Scientific Research from Ministry of Education, Science and Culture of Japan is greatly acknowledged.

References

[1] P. Lagarde and H. Dexpert, Adv. Phys. 33 (1984) 567.
[2] T. Yikegaki, H. Shibata, S. Takatoh, T. Fujikawa and S. Usami, Phys. Scripta 41 (1990) 185.
[3] T. Yikegaki, H. Shibata, K. Takada, S. Takatoh, T. Fujikawa and S. Usami, Vacuum 41 (1990) 352.
[4] B.P. Hollebone, A.T. Wen, T. Tyliszczak and A.P. Hitchcock, J. Electron. Spectry. 51 (1990) 661.
[5] P. Aebi, M. Erbudak, F. Vanini, D.D. Vvedensky and G. Kostorz, Phys. Rev. B 41 (1990) 11760; B 42 (1990) 5369.
[6] T. Fujikawa, S. Takatoh and S. Usami, Japan. J. Appl. Phys. 27 (1988) 348.

[7] B. Luo and J. Urban, Surf. Sci. 239 (1990) 235.
[8] M. DeCrescenzi, L. Lozzi, P. Picozzi, S. Santucci, M. Benfatto and C.R. Natoli, Surf. Sci. 211/212 (1989) 534.
[9] M. DeCrescenzi, L. Lozzi, P. Picozzi, S. Santucci, M. Benfatto and C.R. Natoli, Phys. Rev. B 39 (1989) 8409.
[10] T. Fujikawa and L. Hedin, Phys. Rev. B 40 (1989) 11507.
[11] T. Fujikawa, J. Phys. Soc. Japan 60 (1991) 3904; Surf. Sci. 269/270 (1992) 55.
[12] For example, T.M. Hayes and J.B. Boyce, *Solid State Physics*, Vol. 37, eds. H.E. Ehrenreich, F. Seitz and D. Turnbull (1982) p. 173.
[13] T. Yikegaki, T. Hayashi, T. Enokijima, S. Takatoh, K. Araki, J. Tsukashima and T. Fujikawa, Japan. J. Appl. Phys. (1993), in press.
[14] M. Tomellini and P. Ascarelli, Solid State Commun. 72 (1989) 371.
[15] T. Fujikawa, S. Takatoh and S. Usami, Japan. J. Appl. Phys. 28 (1989) 1683.
[16] T. Yikegaki, N. Yiwata, T. Fujikawa and S. Usami, J. Appl. Phys. 29 (1990) 1362.